Cancer Chemotherapy and Pharmacology (2019) 84:105–116
https://doi.org/10.1007/s00280-019-03854-x

ORIGINAL ARTICLE

Orally administered salecan ameliorates methotrexate-induced intestinal mucositis in mice

Yan Gao[1] · Qi Sun[1] · Xiao Yang[1] · Weiling Lu[1] · Yang Zhao[1] · Wenhao Ge[1] · Yunxia Yang[1] · Xi Xu[1] · Jianfa Zhang[1]

Received: 3 February 2019 / Accepted: 2 May 2019 / Published online: 8 May 2019

Abstract

Purpose Methotrexate (MTX) is a widely used cancer chemotherapy agent. The efficacy of MTX is often limited by serious side effects, such as intestinal mucositis. The aim of this study was to evaluate the protective effect of water-soluble β-glucan salecan on MTX-induced intestinal toxicity in mice.

Methods Intestinal mucositis was induced in C57BL/6 mice by intraperitoneal injection of MTX for two consecutive days. Mice were orally administrated with saline or salecan for 6 days before MTX injection and continued to the end of the study. Several histological and biochemical parameters were measured in the jejunum.

Results Orally administration of salecan improved the severity of intestinal mucositis in a dose-dependent manner, as evidenced by the well-maintained mucosal architecture and body weight in salecan-treated groups. Salecan treatment inhibited MTX-induced oxidative stress and effectively scavenged free radicals both in vitro and in vivo. Metabolomics analysis revealed that salecan treatment reversed the intestinal metabolic profiling changes in mice with MTX-induced mucositis. Salecan treatment modulated the innate immunity through the regulation of TLR and Dectin1 expression in the jejunum, thus protecting mice from MTX-induced intestinal damage.

Conclusions Salecan has potential advantages in the treatment of MTX-induced intestinal mucositis, and its protective effect is mainly attributed to its antioxidant and immunomodulatory properties.

Keywords Methotrexate · Intestine mucositis · Salecan · Antioxidant · Metabonomics

Introduction

Methotrexate (MTX) is widely used as a cytotoxic chemotherapeutic agent for rheumatoid arthritis, leukemia and other malignancies [1]. As a structural analog of folic acid, the effect of MTX is attributed to its ability to inhibit dihydrofolate reductase, affect thymidylate synthesis and DNA synthesis [2]. The efficacy of MTX treatment is often limited by severe side effects, because the cytotoxic of MTX is not only on cancer cells but also on rapid proliferation cells such as gastrointestinal mucosal cells [3]. Intestinal mucositis, which occurs in forty percent of cancer patients after a standard dose of MTX treatment, is one of the most serious side effects. Intestinal mucositis can lead to malabsorption and diarrhea, resulting in anorexia and body weight loss [4]. Ultimately, these side effects can destroy the nutritional status of patients, interrupt the chemotherapy regimen, and impair patients' life quality.

It has been demonstrated that the production of reactive oxygen species (ROS) plays an important role in the initiation and progression of MTX-induced gastrointestinal mucositis [5, 6]. Some studies have shown the beneficial effects of using MTX in combination with antioxidants such as vitamin A and *N*-acetylcysteine [7, 8]. Recently, the microbiota and innate immunity in the small intestine has attracted significant attention in the investigation for the pathobiology of mucositis [9]. Recent years, β-glucans are the most extensively studied polysaccharides with a lot of beneficial biological properties. There is evidence suggesting that β-glucans have antioxidant, antivirus, antitumor and immunomodulatory activities [10, 11]. These properties,

Electronic supplementary material The online version of this article (https://doi.org/10.1007/s00280-019-03854-x) contains supplementary material, which is available to authorized users.

✉ Jianfa Zhang
jfzhang@mail.njust.edu.cn

[1] Center for Molecular Metabolism, Nanjing University of Science and Technology, 200 Xiaolingwei, Nanjing 210094, Jiangsu, People's Republic of China

particularly antioxidant and immunomodulatory effects, suggest that β-glucan may have the potential to protect patients from the side effects of MTX. Salecan is a non-toxic water-soluble β-glucan with a wide range of biological properties, such as reducing lipid peroxidation, attenuating the symptoms of drug-induced constipation, and alleviating dextran sulfate sodium-induced colitis [12, 13]. It has excellent rheological properties and can be used in food industry as food additive [14]. The antioxidant, immunomodulatory, and gastrointestinal protective properties make salecan an ideal nutritional supplement for the treatment of MTX-induced intestinal injury. The aim of this study was to evaluate the protective effect of salecan on MTX-induced intestinal mucositis.

Materials and methods

Chemicals and reagents

Salecan was extracted from the fermentation broth of *Agrobacterium* sp. ZX09 (CCTCC no. M2010020) as described previously [14]. Commercial salecan was purchased from Karroten Scientific (Nanjing, China) with an average molecular weight of 2×10^6. The content of β-glucan in the commercial purified salecan was more than 99%. MTX was purchased from TCI Co. (TCI Shanghai, China, Lot. VUONB-SR).

Animals and experimental design

Male C57BL/6 mice of 7 weeks old were purchased from the Model Animal Research Center of Nanjing University (Nanjing, China). All animals were housed in a temperature- and humidity-controlled room under a 12/12 h light/dark cycle and had free access to tap water and food. All animal care and use procedures were approved by the Institutional Animal Care and Use Committee of Nanjing University of Science and Technology, and were performed according to the Chinese Guidelines for the Care and Use of Laboratory Animals (GB/T 35892-2018).

The induction of experimental intestinal mucositis in mice was previously described by Chang [15]. Mice were randomly assigned into five groups that contained 6 mice in each group. The groups were treated as follows: Control group, mice received saline orally for 10 days and injected with saline intraperitoneally on the 7th and 8th day; Salecan control group, mice received gavage of salecan (40 mg/kg body weight) dissolved in saline for 10 days; MTX group, mice received saline orally for 10 days and injected with 20 mg/kg MTX intraperitoneally on day 7 and day 8; Two salecan-treated groups, mice received gavage of salecan (20 mg/kg body weight for low-dose salecan group and 40 mg/kg body weight for high-dose salecan group) dissolved in saline for 10 days and injected with MTX (20 mg/kg body weight) intraperitoneally on day 7 and day 8. Throughout the experiment, each mice was weighed every day and the feeding state of each mice was recorded. At the end of day 10, all mice were sacrificed, and tissue samples were collected and stored at − 80 °C until use.

Histological analysis

For histological assessments, jejunum samples were dissected, rinsed with ice-cold phosphate buffer saline (PBS), immediately fixed in 10% formalin for 24 h, and embedded in paraffin. The tissues were cut into 5 μm sections, stained with hematoxylin and eosin (H&E), and then examined under a light microscope. Average villus height and crypt depth were measured on 20 well-oriented villi and crypt per section using digitalized images obtained with a digital camera (Nikon Eclipse 80i, Japan).

In vitro cytotoxicity assay

B16F10 cells were maintained in DMEM supplemented with 10% fetal bovine serum (FBS) and 1% penicillin–streptomycin with 5% CO_2 at 37 °C. The cells were treated with MTX and salecan at different dosage. Cell viability was determined with 3-[4, 5-dimethylthiazol-2-yl]-2, 5 diphenyl tetrazolium bromide (MTT) methods.

Biochemical analysis

For biochemical analysis, the jejunum samples were removed, washed and homogenized with ice-cold PBS. Intestinal malonaldehyde (MDA) and glutathione (GSH) levels, catalase (CAT), superoxide dismutase (SOD) and glutathione peroxidase (GPx) activities were determined with commercial analysis kits (Jiancheng Biology Research Center, Nanjing, China) following the manufacturer's instruction.

RNA isolation and quantitative real-time PCR

Total RNA was extracted from the jejunum using Karrol reagent (Karroten Scientific, Nanjing, China) following the manufacturer's instruction. Reverse transcript reaction was performed with a commercial reverse-transcription enzyme (Invitrogen, Carlsbad, CA) according to the manufacturer's instruction. Quantitative real-time PCR was carried out with an ABI 7300 Plus real-time PCR system. The amplification was carried out in a 20 μl reaction volume containing 1 × SYBRGreen PCR Master Mix (10 μl, Toyobo, Osaka, Japan), primers (0.5 μl of each), diluted cDNA (3 μl), and ddH_2O (6 μl). The thermocycling conditions were as follows:

incubation for 10 min at 95 °C, followed by denaturation for 15 s at 95 °C, annealing and extension at 60 °C for 60 s. PCR amplification consisting of 35 cycles was conducted. All samples were run in triplicate. The primers used in this study were listed in Supplementary Table 1. Relative expression in comparison with that of *Gapdh* was calculated using the comparative computed tomography method.

^{1}H NMR sample preparation and ^{1}H NMR spectroscopy

NMR samples were prepared according to the method described by Beckonert et al. [16]. ^{1}H NMR spectra were manually phased and baseline corrected with Topspin software (version 3.0, Bruker Biospin, Germany) and referenced to TSP at 0.0 ppm. Then the data were automatically exported to ASCIIfiles using MestReNova (version 8.0.1, Mestrelab Research SL), and subsequently imported into the open source software R for further phase and baseline correction and peak alignment. The NMR data were binned, probabilistic quotient normalized, mean centered and Pareto scaled before multivariate statistical analysis [17]. Different metabolites in the ^{1}H NMR spectra of the jejunum extracts were identified by the software Chenomx NMR suite 7.7 (Chenomx Inc, Edmonton, AB, Canada). A supervised method OSC-PLS-DA was applied to maximize covariance between the NMR data and the response variable [18]. Color-coded loading plots were constructed to reveal variables that contributed to the group separation. The fold-change values of metabolites and their associated p values corrected by Benjamini and Hochberg-adjusted method were calculated and visualized in colored tables [19].

Free radical scavenging activity assay

The 2, 2-diphenyl-1-picrylhydrazyl (DPPH), superoxide anion and hydroxyl radical scavenging activities of salecan were determined based on methods previously described by Dok-Go et al. [20], Marklund et al. [21], and Smirnoff and Cumbes [22], respectively. The free radical scavenging activities of salecan were calculated according to the following equation: Scavenging activity $(\%) = (1 - A_S/A_C) \times 100$, where A_S and A_C are the absorbance in the presence or absence of salecan.

ROS measurements

The ROS level in jejunum was assessed using the ROS-sensitive fluorescence indicator 2, 7′-dichlorofluorescin-diacetate (DCFH-DA) as previously described with slight modification [23]. Briefly, jejunum tissues were homogenized with ice-cold PBS and diluted to obtain a concentration of 5 mg/ml. The homogenates were centrifuged to collect the supernatant. Subsequently, the fluorescence probe DCFH-DA (Jiancheng Biology Research Center, Nanjing, China) was added to the supernatant, and they were incubated together at 37 °C for 30 min. The fluorescence intensity of the DCF product was measured using a spectrofluorimeter with excitation at 484 nm and emission at 530 nm. Results are expressed as the relative DCF fluorescence intensity.

Statistical analysis

Statistical analysis was carried out with GraphPad Prism 5.0 software (San Diego, CA, USA). Groups of data are presented as mean ± SEM. One-way ANOVA plus post hoc Tukey test or two-tail paired t test was used to evaluate the statistical significance between groups. The following terminology is used to denote the statistical significance: $^*p < 0.05$, $^{**}p < 0.01$.

Results

Salecan ameliorated MTX-induced intestinal mucositis

To verify that MTX caused intestinal mucositis, we microscopically examined the architecture and integrity of the jejunum in different groups. As shown in Fig. 1a (100× magnification) and Fig. 1b (400× magnification), flattened villi, atrophic epithelium and increased number of blood vessels in the stroma were observed in the jejunum sections of mice of MTX group. In contrast, the mucosal architecture was well preserved in the low-dose salecan-treated group (MTX + LS group) and high-dose salecan-treated group (MTX + HS group) (Fig. 1a, b). As expected, the architecture of the jejunum from mice of the salecan control group was normal, no histological damage was observed (Fig. 1a, b). In addition, MTX treatment resulted in a shortened villus height (Fig. 1c) and a shallowed crypt depth (Fig. 1d) as compared with the control group. Administration of salecan prevented the shortening of villus height (Fig. 1c) and shallowing of crypt depth (Fig. 1d) in a dose-dependent manner.

Body weight and food intake of each mice were monitored daily during the study. On the 4th day after MTX treatment, the average body weight of mice in MTX group decreased 6% ($p < 0.05$) compared with the starting average group weights (Fig. 1e). Mice in MTX + LS group showed a 3% decrease in average weight after MTX treatment, but the decrease was not statistically significant ($p = 0.12$) (Fig. 1e). Meanwhile, the average body weight of mice in MTX + HS group was 23.3 ± 0.3 g 4 days after MTX injection, which was comparable with the average body weight (23.6 ± 0.5 g) before MTX injection (Fig. 1e). As shown in Fig. 1f, MTX

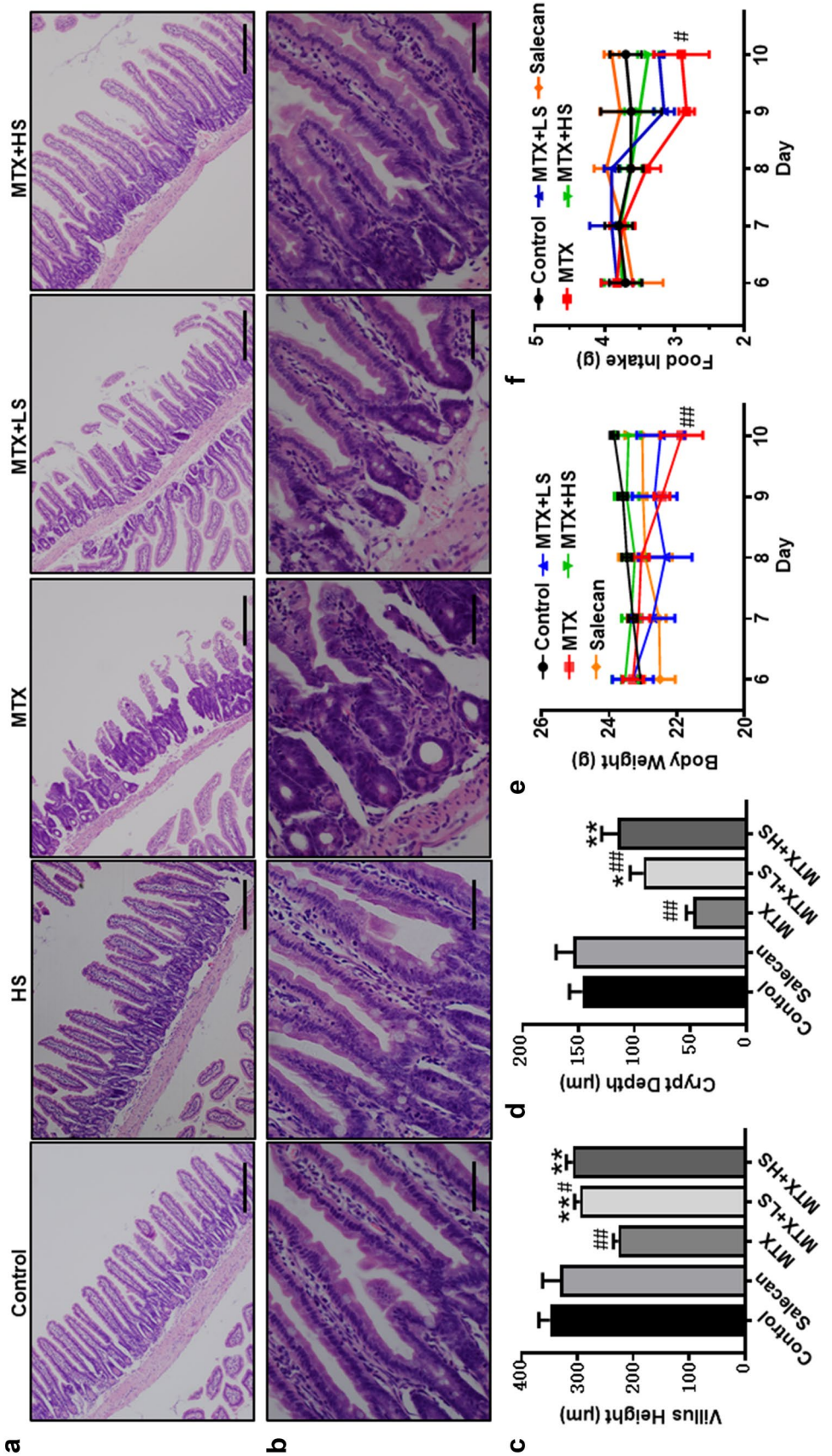

Fig. 1 Salecan attenuated the severity of MTX-induced intestinal mucositis in mice. Representative H&E-stained jejunum sections of different groups were shown at ×100 (**a**) and ×400 (**b**) magnification. The effects of salecan on villus height (**c**) and crypt depth (**d**) were examined. Microscopic measurements of villus and crypt at ×100 magnification were conducted on jejunal sections of each mice. Body weight (**e**) and food intake (**f**) of mice with MTX-induced intestinal mucositis treated with saline or salecan were monitored daily. Scale bar represents 200 μm (**a**) and 50 μm (**b**), respectively. Data are shown as the mean ± SEM, $n = 6$. $^{\#}p < 0.05$, $^{\#\#}p < 0.01$ compared to control group (**c**, **d**); $^{*}p < 0.05$, $^{**}p < 0.01$, compared to MTX group (**c**, **d**); $^{\#}p < 0.05$, $^{\#\#}p < 0.01$ compared to day 6 of the study (**e**, **f**). *LS* low-dose salecan, *HS* high-dose salecan

treatment induced anorexic in mice, and became most severe 48 h after MTX injection. The average food intake of MTX group decreased 21% at the end of the study compared to the average food intake of the day before MTX injection ($p < 0.05$). High-dose salecan treatment significantly relieved the anorexia induced by MTX treatment since the average food intake was not significantly decreased after MTX treatment (Fig. 1f). The average food intake of MTX + LS group mice decreased 16% ($p < 0.05$) at the end of study. Moreover, treated with salecan alone had no significant effect on the body weight and average food intake of mice (Fig. 1e, f), and salecan had no significant effect on the tumor killing activity of MTX (Supplementary Fig. 1). These results indicated that salecan administration successfully alleviated the histopathological damage, anorexia and weight loss caused by MTX treatment in a dose-dependent manner.

Salecan decreased the oxidative stress induced by MTX treatment

To investigate the effects of salecan on the oxidative stress induced by MTX treatment, the contents of MDA, GSH and the activities of SOD, CAT, GPx in the jejunum homogenates were measured. As shown in Fig. 2a, the MDA content in the MTX group increased twofolds ($p < 0.01$) compared with that in the control group, while salecan treatment reduced MDA content to normal level. Furthermore, the SOD (Fig. 2b), CAT (Fig. 2c), and GPx (Fig. 2d) activities in the intestine of mice with MTX-induced mucositis were significantly decreased. Salecan treatment significantly increased these activities in a dose-dependent manner (Fig. 2b–d). A decrease of GSH level in the jejunum was observed in MTX group compared with control group (Fig. 2e). The decreased GSH content was also recovered in the MTX + LS and MTX + HS groups (Fig. 2e).

Effects of salecan on the expression of pro-inflammatory cytokines and genes related to cell apoptosis

Quantitative real-time PCR was carried out to examine the expression of pro-inflammatory cytokines in the jejunum of mice with MTX-induced mucositis. We found that the expression levels of *TNF-α* (Fig. 3a) and *IL-1β* (Fig. 3b) were upregulated in the jejunum of mice with MTX-induced mucositis. Salecan significantly suppressed the expression of *TNF-α* (Fig. 3a) and *IL-1β* (Fig. 3b), and the suppression was dose-dependent. Apoptosis-related genes were also examined in the jejunum. Compared with control mice, the expression level of *Bcl-2* mRNA in the jejunum of mice with MTX-induced mucositis was significantly reduced by 4 times ($p < 0.05$) (Fig. 3c). Meanwhile, salecan treatment significantly increased the down-regulated *Bcl-2* mRNA expression level in a dose-dependent manner (Fig. 3c). Compared to control group, mice in MTX group and salecan-treated groups showed a slight but statistically significant increase in Bax mRNA expression (Fig. 3d). The *Bax:Bcl-2* ratio significantly increased in mice with MTX-induced mucositis, suggesting a decreased enterocyte survival. As expected, salecan treatment reversed the increased *Bax:Bcl-2* ratio in mice with mucositis and increased the enterocyte survival. Administration of salecan alone did not affect the expression of *TNF-α* (Fig. 3a), *IL-1β* (Fig. 3b) and apoptosis related genes (Fig. 3c, d).

Salecan treatment reversed the changes of intestinal metabolic profiles in mice with MTX-induced intestinal mucositis

Metabolomics was used to investigate the effects of salecan treatment on intestinal metabolic profiling of mice with MTX-induced mucositis. Typical ^{1}H NMR spectra for jejunum extracts of control, MTX and MTX + HS groups were exhibited in Supplementary Fig. 2 with metabolites

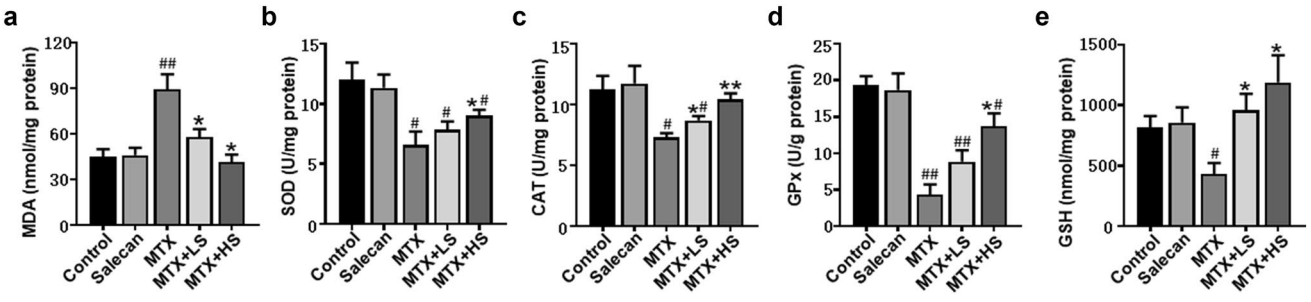

Fig. 2 Effects of salecan treatment on antioxidant markers in the jejunums of mice with MTX-induced mucositis. MDA (**a**) level, SOD (**b**), CAT (**c**), GPx (**d**) activities and GSH (**e**) level were compared between control group, salecan control group, MTX group, and two salecan-treated groups. Data are shown as the mean ± SEM, $n = 6$, $^{\#}p < 0.05$, $^{\#\#}p < 0.01$, compared to control group; $^{*}p < 0.05$, $^{**}p < 0.01$, compared to MTX group. *LS* low-dose salecan, *HS* high-dose salecan

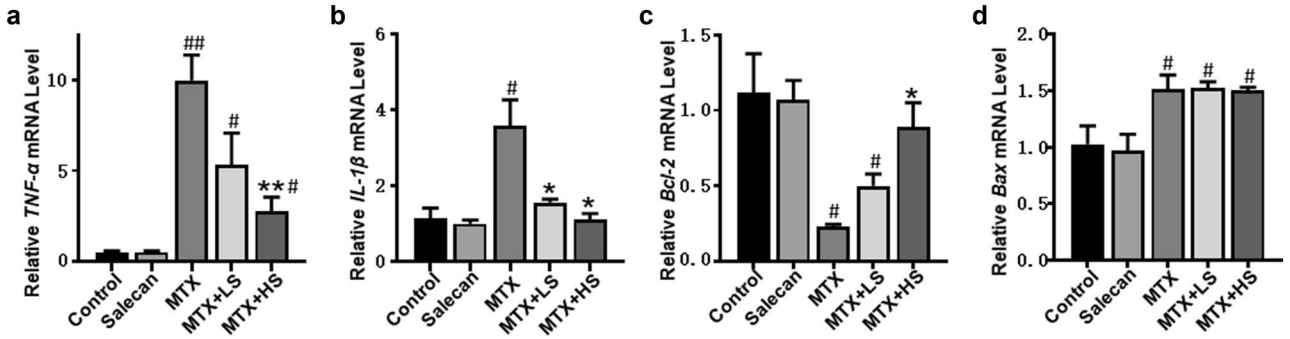

Fig. 3 Effects of salecan on the expression of pro-inflammatory cytokines and apoptosis-related genes. Relative mRNA levels of *TNF-α* (**a**) and *IL-1β* (**b**) in the jejunums of control mice and mice with MTX-induced mucositis treated with saline or salecan. Relative mRNA levels of *Bcl-2* (**c**) and *Bax* (**d**) in the small intestine of mice from different groups. Data are shown as the mean ± SEM, $n = 6$, $^{\#}p < 0.05$, $^{\#\#}p < 0.01$, compared to control group; $^{*}p < 0.05$, $^{**}p < 0.01$, compared to MTX group. *LS* low-dose salecan, *HS* high-dose salecan

Table 1 Metabolites identified from the intestine tissue extracts and their variations of MTX group and MTX + HS group versus control group

Metabolites	Assignments†	ppm	MTX/Control		MTX+HS/Control	
			FC‡	*p*-Value§	FC	*p*-Value
Isoleucine	δCH3 , δCH3, γCH, αCH	0.94(d), 0.96(d), 1.71(m), 3.74(m)	0. 78	***	0. 93	
Leucine	δCH3 , δCH3, γCH, αCH	0.94(d), 0.96(d), 1.71(m), 3.74(m)	0. 74	***	0. 89	*
Valine	γCH3, γCH3	0.98(d), 1.04(d), 2.26(m), 3.61(d)	0. 77	**	0. 94	
Lactate	CH3, CH	1.33(d), 4.11(q)	1. 26	*	0. 99	
Threonine	CH3	1.33(d)	1. 17	*	0. 98	
Alanine	βCH3, αCH	1.48(d), 3.78(q)	0. 83	*	0. 95	
Lysine	δCH2,βCH2,ε-CH2	1.70(m),1.90(m),3.02(t)	0. 79	***	0. 94	
Acetate	CH3, CH	1.92(s)	0. 93		0. 89	*
Glutamate	βCH2, γCH2,αCH	2.14(m),2.36(m),2.50(m), 3.77(t)	1. 27	***	1. 05	
Glutathione	βCH2, γCH2,αCH	2.16(m),2.45(m),3.77(t)	0. 63	*	1. 1	
Succinate	CH2	2.41 (s)	1. 06		0. 92	
Methionine	S-CH3, β-CH2, S-CH2,α-CH	2.14(s),2.16(m),2.65(t),3.86(t)	0. 74	***	0. 91	*
Creatine Phosphate	CH2, CH3	3.03 (s), 3.93 (s)	0. 91		0. 92	
O-Phosphocholine	N(CH3)3	3.23(s)	1. 2		1. 12	*
Taurine	CH2SO3,NCH2	3.25(t),3.42(t)	1. 1		0. 97	
Glycine	HOOC-CH2-NH2	3.57(d)	0. 87	*	1. 03	
Glucose	2H, 3H, 4H, 5H, 6H, 6'H	3.4-3.95 (m), 5.24(d)	1. 22		0. 63	*
Uridine	H5, H6, H1'	5.8(d), 5.82(d), 7.81(d)	0. 56	*	1. 36	*
Inosine	O-CH-N,N-CH=N,N-CH=N	6.10 (d), 8.23 (s), 8.34 (s)	0. 93		1. 22	
Fumarate	CH=CH	6.53(s)	0. 74		0. 73	
Tyrosine	CH, CH	6.90 (d), 7.20 (d)	0. 73	***	0. 88	*
Phenylalanine	CH, CH, CH	7.33 (d), 7.37 (m), 7.43 (m)	0. 82	**	0. 92	
Histidine	N–CH C, N–CH N	7.10 (s), 7.89 (s)	0. 82		1. 03	
3-Methylxanthine	NH=CH-N	8.02(s)	0. 99		1. 13	
Adenosine	CH,NH	8.25(s),8.34(s)	0. 88		0. 88	
AMP	N=CH-N, N=CH-N	8.23(s),8.55(s)	1. 34		1. 03	

FC fold change

†Multiplicity: singlet (s), doublet (d), triplet (t), quartets (q), multiplets (m)

‡Color coded according to the FC, red represents increased and blue represents decreased concentrations in the former group when two groups were compared. Color bar 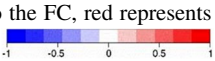

§*p* values: $^{*}p < 0.05$, $^{**}p < 0.01$

labeled. 26 metabolites were identified with their ^{1}H resonances assigned, and the detailed information was presented in Table 1. OSC-PLS-DA analysis was used to evaluate the ^{1}H NMR data and to detect intrinsic clustering and possible outliers. As shown in Fig. 4a, the clustered data points indicated that MTX group were clearly separated from control group and MTX + HS group. The MTX + HS group was not separated from the control group. NMR data of control and MTX group, control and MTX + HS group, were subjected to OSC-PLS-DA analysis and the score plots were shown in Fig. 4b, c, respectively. The s-plot and color-coded loading plots showed variables responsible for the separation of different groups and revealed a large number of altered metabolites that contribute to the separation. In s-plot (Fig. 4d) and color-coded loading plot (Fig. 4e), metabolites in the negative region were reduced in MTX group, while metabolites in the positive region were elevated. The score plot presented separation of the control group and MTX + HS group (Fig. 4c), but the changes in metabolites were not as obvious as in the MTX group (Fig. 4f, g). Notably, most of the decreased metabolites in MTX group were amino acids, suggesting that the amino acid metabolism in mice with MTX-induced mucositis was affected (Fig. 4d). Metabolites related to ROS generation and scavenging were identified as well. Glutathione, the major antioxidant, was significantly decreased in the MTX group and recovered to normal level in the MTX + HS group (Fig. 4d, f), consistent with the result obtained from small intestine homogenates. These results indicated that the intestinal metabolic profiling was

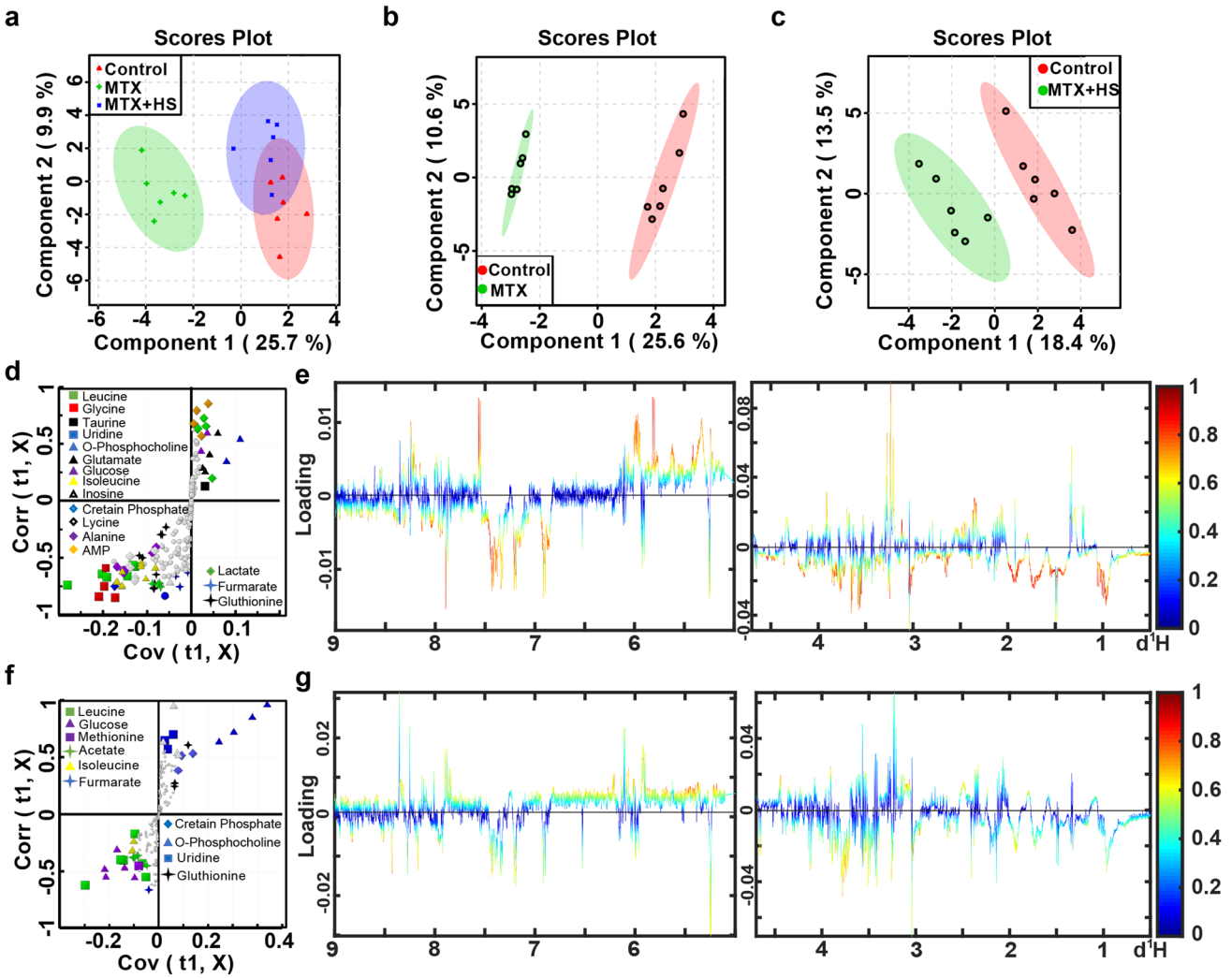

Fig. 4 OSC-PLS-DA analysis of ^{1}H NMR data of small intestine extracts from mice in control group, MTX group, and high-dose salecan group. **a** Score plot of mice from control group, MTX group, and high-dose salecan group. **b** Score plot of control and MTX group. **c** Score plot of control and high-dose salecan group. **d** S-plot of control and MTX group with different metabolites distinguished by color and shown in the legend. **e** Color-coded coefficient loadings plots of the control and MTX group. **f** S-plot of control and high-dose salecan group. **g** Color-coded coefficient loadings plots from ^{1}H NMR spectra of the control and high-dose salecan group

significantly changed by MTX treatment, and high-dose salecan reversed the changes induced by MTX.

Salecan efficiently scavenged free radicals both in vitro and in vivo

Then we investigated that whether salecan have radical scavenging activities in vitro and in vivo. As shown in Fig. 5a, the DPPH scavenging activity of salecan increased with the increasing concentration of salecan. At the concentration of 4 mg/ml, the scavenging rate of salecan against DPPH reached 43.82% (Fig. 5a). The superoxide anion scavenging activity of salecan was measured using the pyrogallol autoxidation method. As shown in Fig. 5b, salecan showed a moderate superoxide anion scavenging activity in a dose-dependent manner. At the concentration of 500 μg/ml, the scavenging rate of salecan was 17.53% (Fig. 5b). Scavenging activity of salecan against hydroxyl radicals was determined using Fenton reaction. According to Fig. 5c, salecan showed good hydroxyl radical scavenging activities. The hydroxyl radical scavenging activity of salecan increased markedly with the increase of concentration. At the concentration of 250 μg/ml, the scavenging rate of salecan for hydroxyl radicals was 60.33% (Fig. 5c), suggesting that salecan is a strong hydroxyl radical scavenger. To evaluate the free radical scavenging activities of salecan in mice with MTX-induced mucositis, ROS levels in the jejunum were measured in all groups. As shown in Fig. 5d, ROS level was significantly increased in the jejunum of MTX-treated mice ($143.3 \pm 9.5\%$, $p < 0.01$) compared to the control group. Salecan treatment significantly reduced the MTX-induced ROS generation ($115.6 \pm 8.9\%$, $p < 0.05$). These results suggested that salecan is efficient in scavenging free radicals both in vitro and in vivo.

Effects of salecan on the expression of toll-like receptor 2 (*TLR2*), *TLR4*, *TLR9*, and *Dectin1* mRNA in mice jejunum

To clarify the effects of salecan on innate immunity in mice jejunum, the mRNA expression of *TLR2*, *TLR4*, *TLR9*, and *Dectin1* were determined. Figure 6 shows different

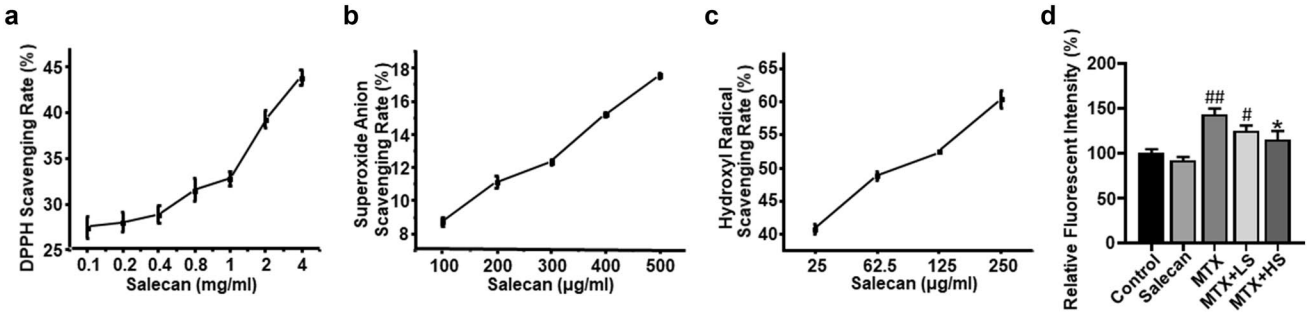

Fig. 5 Salecan efficiently scavenged free radicals both in vitro and in vivo. DPPH (**a**), superoxide anion (**b**) and hydroxyl (**c**) radical scavenging activities of salecan in different concentrations. **d** ROS levels in the jejunum was assessed using the ROS-sensitive fluorescence indicator DCFH-DA and expressed as the relative DCF fluorescence intensity. Data are shown as the mean ± SEM, $n = 6$, $^{\#}p < 0.05$, $^{\#\#}p < 0.01$, compared to control group; $^{*}p < 0.05$, $^{**}p < 0.01$, compared to MTX group. *LS* low-dose salecan, *HS* high-dose salecan

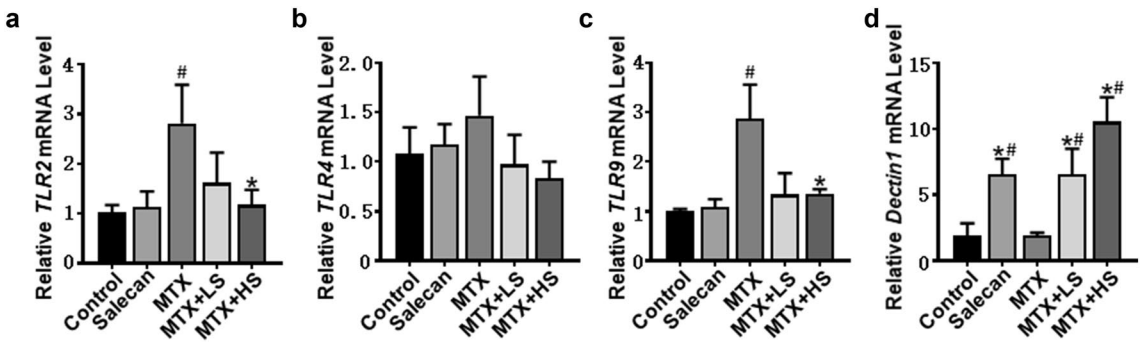

Fig. 6 Effects of salecan on the expression of *TLR2*, *TLR4*, *TLR9*, and *Dectin1* mRNA in mice jejunum. Relative mRNA levels of *TLR-2* (**a**), *TLR-4* (**b**), *TLR-9* (**c**), and *Dectin1* (**d**) in the jejunums of mice. Data are shown as the mean ± SEM, $n = 6$, $^{\#}p < 0.05$, $^{\#\#}p < 0.01$, compared to control group; $^{*}p < 0.05$, $^{**}p < 0.01$, compared to MTX group. *LS* low-dose salecan, *HS* high-dose salecan

expression patterns of *TLR2, TLR4, TLR9*, and *Dectin1* mRNA. Compared with the control group, MTX treatment significantly increased the mRNA expression of *TLR2* (Fig. 6a) and *TLR9* (Fig. 6c) by 2.8 times ($p < 0.05$) and 3 times ($p < 0.05$), respectively. The expression levels of *TLR2* and *TLR9* were significantly reduced in MTX + HS group (Fig. 6a, c). Meanwhile, the expression of *TLR4* was not affected by MTX and salecan treatment (Fig. 6b). *Dectin1* is a non-TLR pattern-recognition receptor that recognizes β-glucan [24]. We found that the mRNA expression of *Dectin1* in the jejunum of salecan-treated mice was significantly increased, and MTX treatment alone had no significant effect on *Dectin1* expression (Fig. 6d), suggesting that *Dectin1* plays an important role in salecan recognition in mice jejunum. These results indicated that salecan can regulate the expression of innate immunity-related genes in mice jejunum.

Discussion

As a chemotherapeutic agent, MTX is widely used in the treatment of various malignancies and rheumatoid arthritis. However, MTX targets both healthy cells and tumor cells without selection [3]. Therefore, the efficiency of MTX is always limited by severe side effects, such as intestinal mucositis. In the present investigation, a well-established mucositis model was used to evaluate the protective effect of salecan on MTX-induced intestinal mucositis. The application of salecan, especially at high dose, significantly relieved the severity of intestinal mucositis induced by MTX administration, as evidenced by the prevented body weight loss and intestinal histopathological damage. We believed that the protective effect of salecan against MTX-induced intestinal mucositis is mainly attributed to its antioxidant and immunomodulatory effects.

The pathogenesis of chemotherapy-induced gastrointestinal mucositis has been reviewed by Sonis et al. [25]. Accordingly, the generation of oxidative stress and reactive oxygen species by chemotherapeutic agents appears to be a primary event in most pathways leading to mucositis. In the initiation phase, MTX treatment initiates intestinal mucositis directly by causing DNA strand breaks and through the generation of ROS. It has been reported that MTX causes intestinal injury via ROS generation [5, 6]. Both increased oxidative stress and decreased antioxidant defenses will occur during MTX treatment [26, 27]. GSH is the major antioxidant protects tissues from ROS and should generally be depleted under oxidative stress. The depletion of GSH level induced by MTX could lead to a reduction in the efficacy of antioxidant enzyme defense system and make cells more sensitive to ROS [28]. SOD, CAT and GPx activities represent the first line of defense against oxidative stress. GPx is known to catalyze the reduction of H_2O_2 into water with GSH as reductant. GST is one of the non-enzymatic antioxidants and contributes majorly to the defense against lipid peroxidation [29]. Naturally, GSH worked as a substrate of both GPx, GR, and GSTs. In our study, MTX treatment depleted the storage of GSH and reduced the activities of major antioxidant enzymes. Salecan efficiently scavenged free radicals both in vivo and in vitro and protected mice from the MTX-induced oxidative stress at the initiation phase.

During the up-regulation phase, ROS damage DNA and cells in the epithelial layer directly and also stimulate secondary mediators such as transcription factors *NF-κB*. Subsequently, the activation of transcription factors resulted in gene up-regulation, including *TNF-α* and *IL-1β*, which can lead to tissue injury and cell apoptosis in the submucosa [25]. In the present study, salecan treatment reduced the MTX-induced up-regulation of *TNF-α* and *IL-1β* mRNA and cell apoptosis. These inhibitory effects of salecan were in accordance with the results of former studies on β-glucans [10, 12].

The influence of MTX is extensive, and all intestinal lesions caused by MTX could have metabolic implications. ^{1}H NMR-based metabolomics analysis revealed that a series of metabolic pathways were disturbed, including pathways involved in oxidative stress generation and clearance, energy metabolism and amino acid metabolism. The decreased glutathione level and increased glutamate level in the intestine of MTX-treated mice were detected by metabolomics analysis, indicating that oxidative stress was up-regulated. MTX-induced high level oxidative stress led to the activation of transcription factors and up-regulation of pro-inflammatory genes. It has been reported that MTX treatment can alter protein metabolism in a specific manner, reduce protein synthesis and an increase proteolysis [30]. Consistent with previous studies, metabolomics analysis revealed that the protein metabolism was impaired in the intestine of mice treated with MTX, as evidenced by the decreased amino acids levels. Salecan treatment reversed most of the metabolite levels changed by MTX, especially amino acids. These results improved our understanding of how MTX treatment alters the metabolic profiles and nutritional status of the small intestine.

It is reported that the human gut mucosal metabolome and microbiome have bi-directional influence, with bacteria influencing metabolites composition and metabolites contributing to microbial community architecture [31]. Several studies indicated that gastrointestinal microbiota may play a critical role in the development of chemotherapy-induced gastrointestinal mucositis [32, 33]. Zhou et al. demonstrated that the composition of the gut microbiome of mice treated with MTX for 14 days was significantly altered [34]. Moreover, microbial metabolic products can contribute to control energy balance and inflammatory responsiveness of the host

[35]. In our study, saelcan treatment reversed the disturbed intestinal metabolic profiling and reduced the expression of pro-inflammatory cytokines. As the intestinal metabolome and microbiome have bi-directional influence, we hypothesized that salecan may help maintain the intestinal microbiome homeostasis during MTX treatment. However, the effect of salecan on intestinal microbiome was not evaluated in this study, which is the limitation of our study. Further studies need to be done to explore the effect of salecan on intestinal microbiome during MTX treatment, and clarify the mechanisms of how salecan affect the intestinal metabolome and microbiome.

It is well known that the gut is an immunological organ in its own right [36]. Initiation of the innate immune response in the intestine is triggered by pathogen-recognition receptors. These receptors recognize molecules of microbial origin, activate pro-inflammatory transcription factors such as *NF-κB*, and play a key role in the innate immune responses [37, 38]. For immune system of the small intestine, β-glucans serve as pathogen-associated molecular pattern that can be recognized by a variety of host-expressed pattern-recognition receptors such as TLRs and Dectin1. TLR signaling has been shown to play a key role in maintaining gut epithelial homeostasis and function in several of pathways which mediate mucositis development [38]. TLRs initiate the innate immune response and the production of pro-inflammatory mediators such as IL-1β and nitric oxide [39]. Kaczmarek and co-workers demonstrated that TLR2 and TLR9 signaling pathways play a central role in the development of doxorubicin-induced intestinal mucositis [40]. In the present study, *TLR2* and *TLR9* mRNA expression was increased in the jejunum of MTX-treated mice. The expression of *TLR2* and *TLR9* can activate a local inflammatory reaction during intestinal mucositis [39]. Salecan treatment reduced the up-regulated expression of *TLR2* and *TLR9* and reduced the inflammatory reaction. It is noteworthy that salecan treatment alone did not activate the expression of TLRs. It is reported that Dectin1 is required for β-glucan recognition and mediates the biological effects of β-glucan [41, 42], and it is a major β-glucan receptor on macrophages [43]. Our results showed that salecan significantly activated the expression of *Dectin1* in the jejunum under pathological condition, indicating that Dectin1 can recognize salecan in the jejunum of mice. TLRs, Dectin1, and other receptors collaborated together to modulate the innate immunity [44], which plays a role in the development of gastrointestinal mucositis. We showed that salecan can modulate the expression of *TLRs* and *Dectin1* in the intestine of mice with MTX-induced mucositis. Former studies have reported that β-glucan can reverse the inhibitory effect of MTX on leukocytes, and attribute to its immunomodulatory effects [45].

In conclusion, orally administered salecan relieved the severity of MTX-induced intestinal mucositis, and the protective effect was mainly attributed to its antioxidant and immunomodulatory properties.

Acknowledgements This work was supported by the grant from National Nature Science Foundation of China (Numbers 31671220, 31471111).

Compliance with ethical standards

Conflict of interest The authors declare no conflict of interest.

References

1. Jolivet J, Cowan KH, Curt GA, Clendeninn NJ, Chabner BA (1983) The pharmacology and clinical use of methotrexate. N Engl J Med 309(18):1094–1104. https://doi.org/10.1056/nejm198311033091805
2. Edwin SL, Chan MD, Bruce N, Cronstein MD (2013) Mechanisms of action of methotrexate. Bull Hosp Jt Dis 71(Suppl 1):S5–S8
3. Grosflam JW, Weinblatt ME (1991) Methotrexate: mechanism of action, pharmacokinetics, clinical indications, and toxicity. Curr Opin Rheumatol 3(3):363–368
4. Pico J-L, Avila-Garavito A, Naccache P (1998) Mucositis: its occurrence, consequences, and treatment in the oncology setting. Oncologist 3(6):446–451
5. Miyazono YG, Horie FT (2004) Oxidative stress contributes to methotrexate-induced small intestinal toxicity in rats. Scand J Gastroenterol 39(11):1119–1127. https://doi.org/10.1080/00365520410003605
6. Gao F, Horie T (2002) A synthetic analog of prostaglandin E1 prevents the production of reactive oxygen species in the intestinal mucosa of methotrexate-treated rats. Life Sci 71(9):1091–1099. https://doi.org/10.1016/S0024-3205(02)01795-2
7. Yuncu ME, Koruk A, Sari M, Bagci I, Inaloz CS (2004) Effect of vitamin A against methotrexate-induced damage to the small intestine in rats. Med Princ Pract 13(6):346–352. https://doi.org/10.1159/000080472
8. Maeda T, Miyazono Y, Ito K, Hamada K, Sekine S, Horie T (2010) Oxidative stress and enhanced paracellular permeability in the small intestine of methotrexate-treated rats. Cancer Chemother Pharmacol 65(6):1117–1123. https://doi.org/10.1007/s00280-009-1119-1
9. van Vliet MJ, Harmsen HJM, de Bont ESJM, Tissing WJE (2010) The role of intestinal microbiota in the development and severity of chemotherapy-induced mucositis. PLoS Pathog 6(5):e1000879. https://doi.org/10.1371/journal.ppat.1000879
10. Kayali H, Ozdag MF, Kahraman S, Aydin A, Gonul E, Sayal A, Odabasi Z, Timurkaynak E (2005) The antioxidant effect of β-Glucan on oxidative stress status in experimental spinal cord injury in rats. Neurosurg Rev 28(4):298–302. https://doi.org/10.1007/s10143-005-0389-2
11. Chen X, Xu X, Zhang L, Zeng F (2009) Chain conformation and anti-tumor activities of phosphorylated (1→3)-β-D-glucan from Poria cocos. Carbohyd Polym 78(3):581–587. https://doi.org/10.1016/j.carbpol.2009.05.019
12. Zhou M, Wang Z, Chen J, Zhan Y, Wang T, Xia L, Wang S, Hua Z, Zhang J (2014) Supplementation of the diet with Salecan attenuates the symptoms of colitis induced by dextran sulphate sodium in mice. Br J Nutr 111(10):1822–1829. https://doi.org/10.1017/S000711451300442X
13. Zhou M, Jia P, Chen J, Xiu A, Zhao Y, Zhan Y, Chen P, Zhang J (2013) Laxative effects of Salecan on normal and two models

of experimental constipated mice. BMC Gastroenterol 13(1):52. https://doi.org/10.1186/1471-230x-13-52
14. Xiu A, Zhou M, Zhu B, Wang S, Zhang J (2011) Rheological properties of Salecan as a new source of thickening agent. Food Hydrocolloids 25(7):1719–1725. https://doi.org/10.1016/j.foodhyd.2011.03.013
15. Chang CJ, Lin CS, Lu CC, Martel J, Ko YF, Ojcius DM, Tseng SF, Wu TR, Chen YY, Young JD, Lai HC (2015) Ganoderma lucidum reduces obesity in mice by modulating the composition of the gut microbiota. Nat Commun 6:7489. https://doi.org/10.1038/ncomms8489
16. Beckonert O, Keun HC, Ebbels TM, Bundy J, Holmes E, Lindon JC, Nicholson JK (2007) Metabolic profiling, metabolomic and metabonomic procedures for NMR spectroscopy of urine, plasma, serum and tissue extracts. Nat Protoc 2(11):2692–2703. https://doi.org/10.1038/nprot.2007.376
17. Craig A, Cloarec O, Holmes E, Nicholson JK, Lindon JC (2006) Scaling and normalization effects in NMR spectroscopic metabonomic data sets. Anal Chem 78(7):2262–2267. https://doi.org/10.1021/ac0519312
18. Pears MR, Cooper JD, Mitchison HM, Mortishire-Smith RJ, Pearce DA, Griffin JL (2005) High resolution 1H NMR-based metabolomics indicates a neurotransmitter cycling deficit in cerebral tissue from a mouse model of Batten disease. J Biol Chem 280(52):42508–42514. https://doi.org/10.1074/jbc.M507380200
19. Benjamini Y, Hochberg Y (1995) Controlling the false discovery rate: a practical and powerful approach to multiple testing. J Roy Stat Soc Ser B (Methodol) 57(1):289–300
20. Dok-Go H, Lee KH, Kim HJ, Lee EH, Lee J, Song YS, Lee Y-H, Jin C, Lee YS, Cho J (2003) Neuroprotective effects of antioxidative flavonoids, quercetin, (+)-dihydroquercetin and quercetin 3-methyl ether, isolated from *Opuntia ficus-indica* var. saboten. Brain Res 965(1):130–136. https://doi.org/10.1016/S0006-8993(02)04150-1
21. Marklund S, Marklund G (1974) Involvement of the superoxide anion radical in the autoxidation of pyrogallol and a convenient assay for superoxide dismutase. Eur J Biochem 47(3):469–474. https://doi.org/10.1111/j.1432-1033.1974.tb03714.x
22. Smirnoff N, Cumbes QJ (1989) Hydroxyl radical scavenging activity of compatible solutes. Phytochemistry 28(4):1057–1060. https://doi.org/10.1016/0031-9422(89)80182-7
23. Shinomol GK, Muralidhara (2007) Differential induction of oxidative impairments in brain regions of male mice following subchronic consumption of Khesari dhal (*Lathyrus sativus*) and detoxified Khesari dhal. Neurotoxicology 28(4):798–806. https://doi.org/10.1016/j.neuro.2007.03.002
24. Brown GD (2006) Dectin-1: a signalling non-TLR pattern-recognition receptor. Nat Rev Immunol 6(1):33–43. https://doi.org/10.1038/nri1745
25. Sonis ST, Elting LS, Keefe D, Peterson DE, Schubert M, Hauer-Jensen M, Bekele BN, Raber-Durlacher J, Donnelly JP, Rubenstein EB, Mucositis Study Section of the Multinational Association for Supportive Care in C, International Society for Oral O (2004) Perspectives on cancer therapy-induced mucosal injury: pathogenesis, measurement, epidemiology, and consequences for patients. Cancer 100(9 Suppl):1995–2025. https://doi.org/10.1002/cncr.20162
26. Chang CJ, Lin JF, Chang HH, Lee GA, Hung CF (2013) Lutein protects against methotrexate-induced and reactive oxygen species-mediated apoptotic cell injury of IEC-6 cells. PLoS One 8(9):e72553. https://doi.org/10.1371/journal.pone.0072553
27. Huang CC, Hsu PC, Hung YC, Liao YF, Liu CC, Hour CT, Kao MC, Tsay GJ, Hung HC, Liu GY (2005) Ornithine decarboxylase prevents methotrexate-induced apoptosis by reducing intracellular reactive oxygen species production. Apoptosis 10(4):895–907. https://doi.org/10.1007/s10495-005-2947-z
28. Jahovic N, Çevik H, Şehirli AÖ, Yeğen BÇ, Şener G (2003) Melatonin prevents methotrexate-induced hepatorenal oxidative injury in rats. J Pineal Res 34(4):282–287. https://doi.org/10.1034/j.1600-079X.2003.00043.x
29. Sheehan D, Meade G, Foley VM, Dowd CA (2001) Structure, function and evolution of glutathione transferases: implications for classification of non-mammalian members of an ancient enzyme superfamily. Biochem J 360(Pt 1):1–16
30. Fijlstra M, Schierbeek H, Voortman G, Dorst KY, van Goudoever JB, Rings EHHM, Tissing WJE (2012) Continuous enteral administration can enable normal amino acid absorption in rats with methotrexate-induced gastrointestinal mucositis. J Nutr 142(11):1983–1990. https://doi.org/10.3945/jn.112.165209
31. McHardy IH, Goudarzi M, Tong M, Ruegger PM, Schwager E, Weger JR, Graeber TG, Sonnenburg JL, Horvath S, Huttenhower C, McGovern DPB, Fornace AJ, Borneman J, Braun J (2013) Integrative analysis of the microbiome and metabolome of the human intestinal mucosal surface reveals exquisite inter-relationships. Microbiome 1(1):17. https://doi.org/10.1186/2049-2618-1-17
32. Stringer AM, Gibson RJ, Bowen JM, Logan RM, Ashton K, Yeoh ASJ, Al-Dasooqi N, Keefe DMK (2009) Irinotecan-induced mucositis manifesting as diarrhoea corresponds with an amended intestinal flora and mucin profile. Int J Exp Pathol 90(5):489–499. https://doi.org/10.1111/j.1365-2613.2009.00671.x
33. Stringer AM, Gibson RJ, Logan RM, Bowen JM, Yeoh ASJ, Hamilton J, Keefe DMK (2009) Gastrointestinal microflora and mucins may play a critical role in the development of 5-fluorouracil-induced gastrointestinal mucositis. Exp Biol Med 234(4):430–441. https://doi.org/10.3181/0810-rm-301
34. Zhou B, Xia X, Wang P, Chen S, Yu C, Huang R, Zhang R, Wang Y, Lu L, Yuan F, Tian Y, Fan Y, Zhang X, Shu Y, Zhang S, Bai D, Wu L, Xu H, Yang L (2018) Induction and amelioration of methotrexate-induced gastrointestinal toxicity are related to immune response and gut microbiota. EBioMed 33:122–133. https://doi.org/10.1016/j.ebiom.2018.06.029
35. Tilg H, Kaser A (2011) Gut microbiome, obesity, and metabolic dysfunction. J Clin Investig 121(6):2126–2132. https://doi.org/10.1172/JCI58109
36. Thorpe DW, Stringer AM, Gibson RJ (2013) Chemotherapy-induced mucositis: the role of the gastrointestinal microbiome and toll-like receptors. Exp Biol Med 238(1):1–6. https://doi.org/10.1258/ebm.2012.012260
37. Santaolalla R, Abreu MT (2012) Innate immunity in the small intestine. Curr Opin Gastroenterol 28(2):124–129. https://doi.org/10.1097/MOG.0b013e3283506559
38. Rakoff-Nahoum S, Paglino J, Eslami-Varzaneh F, Edberg S, Medzhitov R (2004) Recognition of commensal microflora by toll-like receptors is required for intestinal homeostasis. Cell 118(2):229–241. https://doi.org/10.1016/j.cell.2004.07.002
39. Wong DV, Lima-Junior RC, Carvalho CB, Borges VF, Wanderley CW, Bem AX, Leite CA, Teixeira MA, Batista GL, Silva RL, Cunha TM, Brito GA, Almeida PR, Cunha FQ, Ribeiro RA (2015) The adaptor protein Myd88 is a key signaling molecule in the pathogenesis of irinotecan-induced intestinal mucositis. PLoS One 10(10):e0139985. https://doi.org/10.1371/journal.pone.0139985
40. Kaczmarek A, Brinkman BM, Heyndrickx L, Vandenabeele P, Krysko DV (2012) Severity of doxorubicin-induced small intestinal mucositis is regulated by the TLR-2 and TLR-9 pathways. J Pathol 226(4):598–608. https://doi.org/10.1002/path.3009
41. Brown GD, Herre J, Williams DL, Willment JA, Marshall ASJ, Gordon S (2003) Dectin-1 mediates the biological effects of β-Glucans. J Exp Med 197(9):1119–1124. https://doi.org/10.1084/jem.20021890
42. Taylor PR, Tsoni SV, Willment JA, Dennehy KM, Rosas M, Findon H, Haynes K, Steele C, Botto M, Gordon S, Brown GD (2007)

Dectin-1 is required for β-glucan recognition and control of fungal infection. Nat Immunol 8:31–38. https://doi.org/10.1038/ni1408
43. Brown GD, Taylor PR, Reid DM, Willment JA, Williams DL, Martinez-Pomares L, Wong SYC, Gordon S (2002) Dectin-1 is a major β-Glucan receptor on macrophages. J Exp Med 196(3):407–412. https://doi.org/10.1084/jem.20020470
44. Underhill DM (2007) Collaboration between the innate immune receptors dectin-1, TLRs, and Nods. Immunol Rev 219(1):75–87. https://doi.org/10.1111/j.1600-065X.2007.00548.x
45. Sener G, Eksioglu-Demiralp E, Cetiner M, Ercan F, Yegen BC (2006) Beta-glucan ameliorates methotrexate-induced oxidative organ injury via its antioxidant and immunomodulatory effects. Eur J Pharmacol 542(1–3):170–178. https://doi.org/10.1016/j.ejphar.2006.02.056